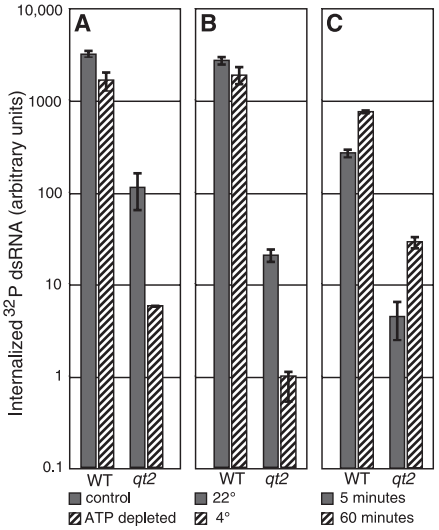

Fig. 4. SID-1 rapidly mediates passive uptake of dsRNA in S2 cells. (**A**) SID-1–mediated dsRNA uptake is resistant to ATP depletion. Cells (4×10^6) were plated in duplicate in 24-well plates in 5 μM oligomycin or dimethyl sulfoxide (DMSO) control for 30 min before addition of dsRNA. Cells were incubated with dsRNA for 1 hour at 22°C, washed once with cold phosphate-buffered saline (PBS), treated with trypsin for 15 min, pelleted, washed in PBS three times, and lysed. Radioactivity in lysates was measured and normalized to total protein content. Washing cells with acidified PBS was as effective as trypsin in removing extracellular label (*3*, *19*). (**B**) SID-1–mediated dsRNA uptake is resistant to reduced temperatures. Cells (4×10^6) were plated in duplicate, allowed to adhere for 30 min at 27°C, then moved to 4°C for 10 min. dsRNA was added, and cells either remained at 4°C or were warmed to 22°C. After 1 hour, both sets of cells were returned to 4°C, washed once with cold PBS, and trypsin was added. Both sets of cells were then moved to 22°C and processed as in (A). (**C**) SID-1–mediated uptake proceeds rapidly. Cells were plated as in (B) before addition of dsRNA and, after either 5 min or 60 min incubation (22°C), were washed and processed in (A).

coproteins. Low-affinity interactions with glycoproteins would be stabilized by increases in avidity that accompany lengthening of a dsRNA molecule. Longer molecules would bind more stably to the cell surface and thereby increase the concentration of dsRNA immediately surrounding the dsRNA channel. Such a discriminatory mechanism would enable organisms to use long dsRNA to systemically silence natural targets, including transposons or viruses, while spatially and temporally confining expression of short dsRNAs, such as regulatory microRNAs (*20*, *21*).

SID-1–mediated dsRNA transport may have numerous functional genomic and therapeutic applications. RNAi screens have been highly effective in *C. elegans* and S2 cells, which readily import dsRNA, whereas transfection-based RNAi screens require substantially more labor (*8*, *12*, *22*). Ectopic SID-1 expression may enable RNAi soaking screens in a number of experimental systems. Perhaps most important, *sid-1* belongs to a previously uncharacterized gene family with members within the human and murine genomes (*2*). Should these genes function similarly to *C. elegans sid-1*, modulation of their activity could enable in vivo use of RNAi to regulate gene expression.

References and Notes

1. A. Fire *et al.*, *Nature* **391**, 806 (1998).
2. W. M. Winston, C. Molodowitch, C. P. Hunter, *Science* **295**, 2456 (2002).
3. Materials and Methods are available as supporting online material at *Science* Online.
4. X. Li, I. Greenwald, *Neuron* **17**, 1015 (1996).
5. T. J. Silhavy, J. R. Beckwith, *Microbiol. Rev.* **49**, 398 (1985).
6. S. M. Hammond, E. Bernstein, D. Beach, G. J. Hannon, *Nature* **404**, 293 (2000).
7. N. Tavernarakis, S. L. Wang, M. Dorovkov, A. Ryazanov, M. Driscoll, *Nature Genet.* **24**, 180 (2000).
8. M. Ramet, P. Manfruelli, A. Pearson, B. Mathey-Prevot, R. A. Ezekowitz, *Nature* **416**, 644 (2002).
9. C. A. Worby, N. Simonson-Leff, J. E. Dixon, *Sci. STKE* **2001**, pl1 (2001).
10. S. M. Elbashir *et al.*, *Nature* **411**, 494 (2001).
11. B. W. Draper, C. C. Mello, B. Bowerman, J. Hardin, J. R. Priess, *Cell* **87**, 205 (1996).
12. L. Lum *et al.*, *Science* **299**, 2039 (2003).
13. D. S. Kwon, G. Gregorio, N. Bitton, W. A. Hendrickson, D. R. Littman, *Immunity* **16**, 135 (2002).
14. A. Shibuya *et al.*, *Nature Immunol.* **1**, 441 (2000).
15. K. Han *et al.*, *Mol. Cells* **12**, 267 (2001).
16. S. D. Conner, S. L. Schmid, *Nature* **422**, 37 (2003).
17. H. Tabara, E. Yigit, H. Siomi, C. C. Mello, *Cell* **109**, 861 (2002).
18. E. Bernstein, A. A. Caudy, S. M. Hammond, G. J. Hannon, *Nature* **409**, 363 (2001).
19. E. H. Feinberg, C. P. Hunter, unpublished data.
20. H. Tabara *et al.*, *Cell* **99**, 123 (1999).
21. V. Ambros, *Cell* **107**, 823 (2001).
22. R. S. Kamath *et al.*, *Nature* **421**, 231 (2003).

23. We wish to thank A. Kiger for pPacPl and advice concerning S2 cells; L. Lum and P. Beachy for cl-8 cells, growth supplements, and technical advice; M. Sutherlin and D. Mootz for critical reading of this manuscript; and P. Beachy and all members of the Hunter laboratory for helpful comments and suggestions. Supported by The Beckman Young Investigators Foundation and the National Science Foundation (MCB-01110452).

Supporting Online Material

www.sciencemag.org/cgi/content/full/301/5639/1545/DC1
Materials and Methods
Fig. S1
Tables S1 and S2
References

22 May 2003; accepted 31 July 2003

Orientation of Asymmetric Stem Cell Division by the APC Tumor Suppressor and Centrosome

Yukiko M. Yamashita,[1] D. Leanne Jones,[1] Margaret T. Fuller[1,2]*

Stem cell self-renewal can be specified by local signals from the surrounding microenvironment, or niche. However, the relation between the niche and the mechanisms that ensure the correct balance between stem cell self-renewal and differentiation is poorly understood. Here, we show that dividing *Drosophila* male germline stem cells use intracellular mechanisms involving centrosome function and cortically localized Adenomatous Polyposis Coli tumor suppressor protein to orient mitotic spindles perpendicular to the niche, ensuring a reliably asymmetric outcome in which one daughter cell remains in the niche and self-renews stem cell identity, whereas the other, displaced away, initiates differentiation.

Adult stem cells maintain populations of highly differentiated but short-lived cells such as skin, intestinal epithelium, or sperm through a critical balance between alternate fates: Daughter cells either maintain stem cell identity or initiate differentiation (*1*). In *Drosophila* testes, germline stem cells (GSCs) normally divide asymmetrically, giving rise to one stem cell and one gonialblast, which initiates differentiation starting with the spermatogonial transient amplifying divisions. The hub, a cluster of somatic cells at the testis apical tip, functions as a stem cell niche: Apical hub cells express the signaling ligand Unpaired (Upd), which activates the Janus kinase–signal transducers and activators of transcription (JAK-STAT) pathway within GSCs to maintain stem cell identity (*2*, *3*).

Analysis of dividing male GSCs by expression of green fluorescent protein (GFP)–α-tubulin in early germ cells revealed that in 100% of the dividing stem cells observed ($n > 500$), the mitotic spindle was oriented perpendicular to the hub-GSC interface throughout mitosis, with one spindle pole positioned within the crescent where the GSC contacted the hub (Fig. 1, A to C, and fig. S1). Stem cell division was rare, averaging one dividing stem cell observed per 5 to 10

[1]Department of Developmental Biology, [2]Department of Genetics, Stanford University School of Medicine, Stanford, CA 94305–5329, USA.

*To whom correspondence should be addressed. E-mail: fuller@cmgm.stanford.edu

testes (~2% of total stem cells) in 0- to 2-day-old adults. Spindles were not oriented toward the hub in gonialblasts (Fig. 1C).

Drosophila male GSCs maintained a fixed orientation toward the hub throughout the cell cycle, unlike *Drosophila* embryonic neuroblasts or the *Caenorhabditis elegans* P1 cell, in which spindle orientation is established during mitosis by a programmed rotation of the spindle (*5*, *6*). The single centrosome in early interphase GSCs was consistently located adjacent to the hub (Fig. 1D, arrow). After centrosome duplication, one centrosome remained adjacent to the hub, whereas the other migrated to the opposite side of the nucleus (Fig. 1, D to F). The mechanisms responsible for *Drosophila* GSC spindle orientation may differ between sexes. In female GSCs, the spectrosome, a spherical intracellular membranous structure, remains localized next to the apical cap cells, where it may help anchor the spindle pole during mitosis (*7*). In interphase male GSCs, in contrast, the spectrosome was often located to the side, whereas at least one centrosome held the stereotyped position adjacent to the hub (Fig. 1G).

To investigate centrosome function in orientation of male GSCs, we analyzed males that were null mutant for the integral centrosome component *centrosomin* (*cnn*) (*8*, *9*), which is required for normal astral microtubule function (*10*). In *cnn* mutant males, mitotic spindles were not oriented toward the hub in ~30% ($n > 100$) of the dividing GSCs examined (Fig. 2A). In an additional 10 to 20%, spindles were properly oriented, but the proximal spindle pole was no longer closely associated with the cell cortex at the hub-GSC interface and the entire spindle was displaced away from the hub (Fig. 2B). The frequency of spindle orientation defects was highest in metaphase (Fig. 2C). Loss of function of *cnn* also partially randomized the interphase centrosome positioning in male GSCs. In more than 35% of the *cnn* mutant GSCs with duplicated centrosomes that were scored (table S1), neither centrosome was positioned next to the hub (Fig. 2, D and E).

The number of germ cells associated with the hub was increased 20 to 30% in *cnn* mutant males, from an average of 8.94 GSCs per hub in the wild type to 11.89 GSCs per hub in cnn^{HK21}/cnn^{HK21} ($P = 1.3 \times 10^{-8}$) and 10.69 GSCs per hub in cnn^{HK21}/cnn^{mfs3} ($P = 7.2 \times 10^{-6}$) (Fig. 2F and table S1). Hub size was not significantly different in *cnn* compared with wild-type males (table S1). In *cnn* testes with many stem cells, GSCs appeared crowded around the hub and often seemed attached to the hub by only a small region of cell cortex (Fig. 2, G to J). Finite available physical space around the hub may limit the increase in stem cell number in *cnn* mutant males.

As suggested by the increased stem cell number, there were several cases in both live and fixed samples from *cnn* males in which a stem cell that had recently divided with a mitotic spindle parallel to the hub-GSC interface produced two daughter cells that retained contact with the hub (Fig. 2K), a finding that was not observed in the wild type. We also observed GSCs dividing with a misoriented/detached spindle that lost attachment to the hub (Fig. 2L), probably explaining the mild increase in stem cell number relative to the frequency of misoriented spindles.

The normal close attachment of one spindle pole to a region of the GSC next to the hub and the effects of *cnn* mutants on centrosome and spindle orientation suggest that a specialized region of the GSC cell cortex touching the hub might provide a polarity cue toward which astral microtubules from the centrosome and spindle pole orient. High levels of DE-cadherin (fly epithelial cadherin) and Armadillo (Arm; fly β-catenin) colocalized at the hub-GSC interface (Fig. 3, A to C), as well as at the interface between adjacent hub cells, marked by high levels of Fas III (Fig. 3C). High levels of DE-cadherin and Arm were not detected around the rest of the GSC surface. Forced expression of DE-cadherin–GFP specifically in early germ cells (*4*) confirmed that DE-cadherin in GSCs colocalized to the hub-GSC interface (Fig. 3D).

DE-cadherin and Armadillo at the hub-GSC interface may provide an anchoring platform for localized concentration of Apc2, one of two *Drosophila* homologs of the mammalian tumor suppressor gene Adenomatous Polyposis Coli (*APC*) (*11*, *12*), which in turn may anchor astral microtubules to orient centrosomes and the spindle. Immunofluorescence analysis revealed Apc2

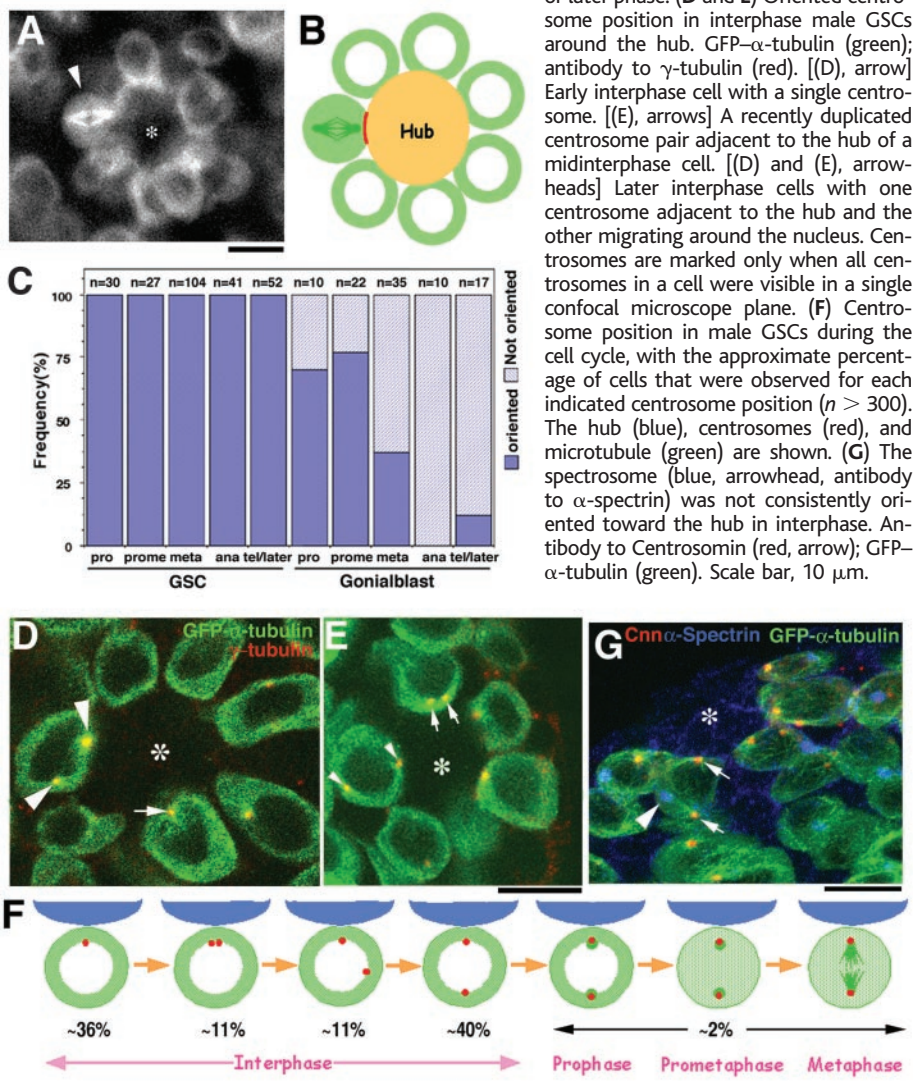

Fig. 1. Male GSCs orient toward the hub throughout the cell cycle. (**A**) In the apical tip of a *Drosophila* testis, male GSCs are visualized with *nos-gal4-VP16/upstream activating sequence (UAS)–GFP–α-tubulin (4)*. GSCs form a rosette of GFP-positive cells around and touching the GFP-negative hub (*). (Arrowhead) A GSC undergoing mitosis. (**B**) A schematic of GSCs (green) surrounding the hub (orange). The proximal spindle pole in GSCs always associated with the hub-GSC interface (red line), with the other pole on the opposite side. (**C**) Spindles oriented perpendicular to the hub in GSCs but not gonialblasts. Pro, prophase; prome, prometaphase; meta, metaphase; and, anaphase; tel/later, telophase or later phase. (**D** and **E**) Oriented centrosome position in interphase male GSCs around the hub. GFP–α-tubulin (green); antibody to γ-tubulin (red). [(D), arrow] Early interphase cell with a single centrosome. [(E), arrows] A recently duplicated centrosome pair adjacent to the hub of a midinterphase cell. [(D) and (E), arrowheads] Later interphase cells with one centrosome adjacent to the hub and the other migrating around the nucleus. Centrosomes are marked only when all centrosomes in a cell were visible in a single confocal microscope plane. (**F**) Centrosome position in male GSCs during the cell cycle, with the approximate percentage of cells that were observed for each indicated centrosome position ($n > 300$). The hub (blue), centrosomes (red), and microtubule (green) are shown. (**G**) The spectrosome (blue, arrowhead, antibody to α-spectrin) was not consistently oriented toward the hub in interphase. Antibody to Centrosomin (red, arrow); GFP–α-tubulin (green). Scale bar, 10 μm.

protein localized to the hub-GSC interface (Fig. 3, E to H). In *apc2* mutant males, we observed GSCs with mispositioned centrosomes (16 to 21%, $n > 100$), misoriented spindles (10 to 14%, $n > 35$) (Fig. 3I and table S1), or detached spindles (8 to 11%, $n > 35$). Both the average number of stem cells (11 to 12 per testis; $n > 100$) and hub diameter increased in *apc2* mutant males compared with that of the wild type. Unlike in *cnn* mutants, GSCs did not appear crowded around the hub in *apc2* males, perhaps as a result of the enlarged hub.

The second *Drosophila APC* homolog, *apc1*, may also contribute to normal orientation of the interphase centrosome and mitotic spindle. Apc1 protein localized to centrosomes in GSCs (Fig. 3J) and spermatogonia during late G_2/prophase, after centrosomes were fully separated but before nuclear envelope breakdown. Apc1 was not detected at centrosomes from prometaphase to telophase. Spindle orientation (~20%, $n > 15$) and centrosome position (22 to 45%, $n > 100$) were perturbed in GSCs from *apc1* males (Fig. 3K and table S1), and the number of stem cells per testis and the diameter of the hub both slightly increased in *apc1* mutant testes compared with those of the wild type (table S1).

We propose that the reliably asymmetric outcome of male GSC divisions is controlled by the concerted action of (i) extrinsic factor(s) from the niche that specify stem cell identity, and (ii) intrinsic cellular machinery acting at the centrosome and a specialized region of the GSC cortex located at the hub-GSC interface to orient the cell division plane with respect to the signaling microenvironment (Fig. 3L). Astral microtubules emanating from the centrosome

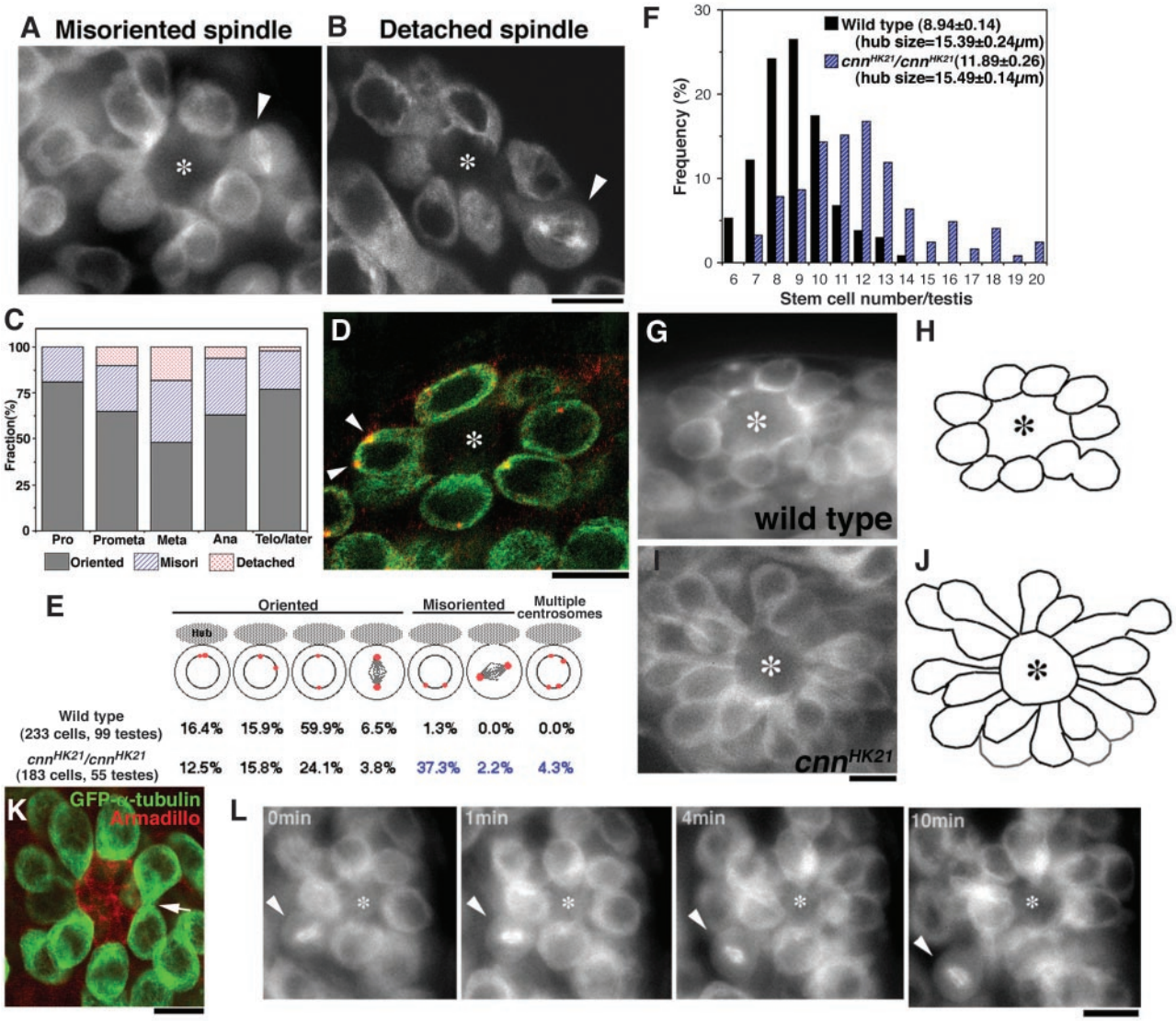

Fig. 2. Misoriented spindle and centrosomes and increased stem cell number in *cnn* mutant testes. (**A** and **B**) GSCs around the hub (*) from cnn^{HK21} homozygous males. [(A), arrowhead] A misoriented spindle. [(B), arrowhead] A detached spindle. (**C**) Frequency of abnormal spindles in cnn^{HK21} male GSCs. Misori, misoriented. (**D**) Confocal image of cnn^{HK21} male GSCs showing mispositioned centrosomes (arrowheads). GFP–α-tubulin (green); antibody to γ-tubulin (red). (*) Hub. (**E**) Frequency of GSCs with mispositioned centrosomes. Only cells with two visible duplicated centrosomes were scored. Cells were counted as having mispositioned centrosomes if neither centrosome was located near the interface with the hub. (**F**) Distribution of stem cell number in the wild-type compared with cnn^{HK21} mutant testes, with average stem cell number (±SE). (**G** and **I**) Male GSCs around the hub (*) visualized live with *nos-Gal4-VP16*/UAS-GFP–α-tubulin in (G) the wild type and (I) cnn^{HK21}. (**H** and **J**) Trace of GSCs. The thicker focal plane of the regular fluorescent microscope used allowed visualization of almost all the stem cells in a single image. Gray outlines in (J) indicate cells contacting the hub in a different focal plane. (**K**) A GSC in a cnn^{HK21}/cnn^{mfs3} testis dividing so that both daughter cells retain attachment to the hub. (Arrow) cytoplasmic bridge. GFP–α-tubulin (green); antibody to Armadillo (red). (**L**) Time-lapse series of a dividing GSC with detached and misoriented spindle (arrowhead) in cnn^{HK21}, showing loss of cell attachment to hub. Scale bar, 10 μm.

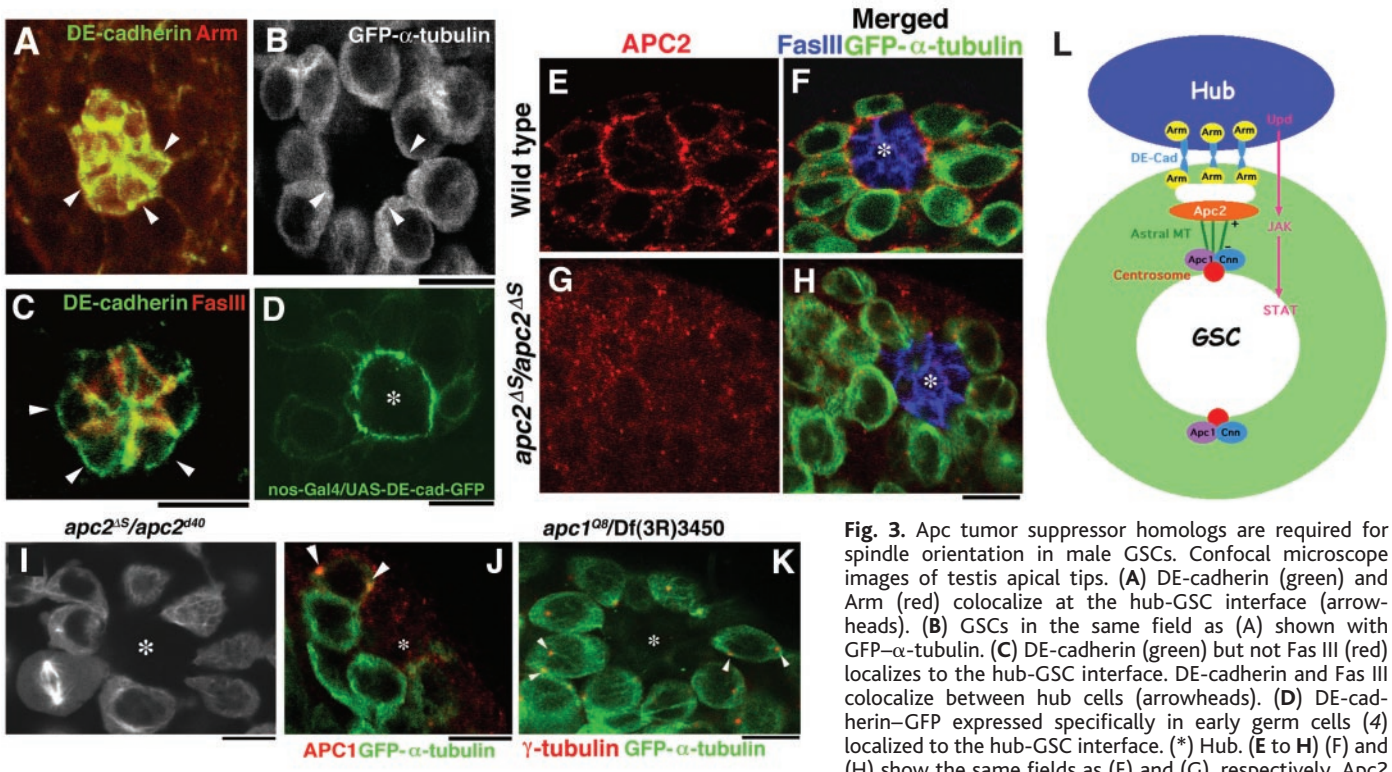

Fig. 3. Apc tumor suppressor homologs are required for spindle orientation in male GSCs. Confocal microscope images of testis apical tips. (**A**) DE-cadherin (green) and Arm (red) colocalize at the hub-GSC interface (arrowheads). (**B**) GSCs in the same field as (A) shown with GFP–α-tubulin. (**C**) DE-cadherin (green) but not Fas III (red) localizes to the hub-GSC interface. DE-cadherin and Fas III colocalize between hub cells (arrowheads). (**D**) DE-cadherin–GFP expressed specifically in early germ cells (*4*) localized to the hub-GSC interface. (*) Hub. (**E** to **H**) (F) and (H) show the same fields as (E) and (G), respectively. Apc2 localized to the hub-GSC interface in the wild type [(E) and (F)] but not in $apc2^{\Delta S}/apc2^{\Delta S}$ [(G) and (H)], $apc2^{\Delta S}/apc2^{d40}$, $apc2^{\Delta S}/apc2^{N175K}$, or $apc2^{d40}/apc2^{N175K}$ (not shown). Antibody to Apc2 (red); GFP–α-tubulin (green); antibody to Fas III (blue). (*) Hub. (**I**) Misoriented spindle in $apc2^{\Delta S}/apc2^{d40}$ (*nos-Gal4-VP16*/UAS-GFP–α-tubulin). (*) Hub. (**J**) Apc1 localized to centrosomes in G_2/prophase male GSCs (arrowheads). Anti-body to Apc1 (red); GFP–α-tubulin (green). (*) Hub. (**K**) Mispositioned centrosomes (arrowheads) in an $apc1^{Q8}/Df(3R)3450$ mutant testis. (*) Hub. Antibody to γ-tubulin (red); GFP–α-tubulin (green). (**L**) Model for asymmetric stem cell division in *Drosophila* male GSCs. Scale bar, 10 μm.

may be captured by a localized protein complex including Apc2 at the GSC cortex where it interfaces with the hub (Fig. 3L), similar to the way in which cortical Apc2 may orient mitotic spindles in the syncytial embryo (*13*) or epithelial cells (*14*).

Mechanisms that orient the mitotic spindle by attachment of astral microtubules to specific cortical sites may be evolutionally conserved. In budding yeast, spindle orientation is controlled by capture and tracking of cytoplasmic microtubules to the bud tip (*15*, *16*), dependent on Kar9, which has weak sequence similarity to APC proteins (*17*, *18*). Kar9 has been localized to the spindle pole body (*19*) and the cell cortex of the bud tip (*20*, *21*), reminiscent of the localization of *Drosophila* Apc1 at centrosomes and Apc2 at the cell cortex (*22*).

Polarization of *Drosophila* male GSCs toward the hub could result simply from the geometry of cell-cell adhesion. GSCs appear to be anchored to the hub in part through localized adherens junctions (*23*). Homotypic interactions between DE-cadherin on the surface of hub cells and male GSCs could concentrate and stabilize a patch of DE-cadherin. The resulting localized DE-cadherin cytoplasmic domains could then provide localized binding sites for β-catenin and Apc2 at the GSC cortex (Fig. 3L). Although binding of E-cadherin and APC to β-catenin is thought to be mutually exclusive (*24*), APC could be anchored at the cortical patch through the actin cytoskeleton, which in turn could interact with β-catenin/α-catenin.

Orientation of stem cells toward the niche appears to play a critical role in the mechanism that ensures a reliably asymmetric outcome of *Drosophila* male GSC divisions, consistently placing one daughter within the reach of short-range signals from the hub and positioning the other away from the niche. Oriented stem cell division may be a general feature of other stem cell systems, helping maintain the correct balance between stem cell self-renewal and initiation of differentiation throughout adult life.

References and Notes

1. F. M. Watt, B. L. Hogan, *Science* **287**, 1427 (2000).
2. A. A. Kiger, D. L. Jones, C. Schulz, M. B. Rogers, M. T. Fuller, *Science* **294**, 2542 (2001).
3. N. Tulina, E. Matunis, *Science* **294**, 2546 (2001).
4. Materials and methods are available as supporting material on *Science* Online.
5. J. A. Kaltschmidt, C. M. Davidson, N. H. Brown, A. H. Brand, *Nature Cell Biol.* **2**, 7 (2000).
6. A. A. Hyman, J. G. White, *J. Cell Biol.* **105**, 2123 (1987).
7. W. Deng, H. Lin, *Dev. Biol.* **189**, 79 (1997).
8. J. G. Heuer, K. Li, T. C. Kaufman, *Development* **121**, 3861 (1995).
9. K. Li, T. C. Kaufman, *Cell* **85**, 585 (1996).
10. T. L. Megraw, L. R. Kao, T. C. Kaufman, *Curr. Biol.* **11**, 116 (2001).
11. X. Yu, L. Waltzer, M. Bienz, *Nature Cell Biol.* **1**, 144 (1999).
12. B. M. McCartney *et al.*, *J. Cell Biol.* **146**, 1303 (1999).
13. B. M. McCartney *et al.*, *Nature Cell Biol.* **3**, 933 (2001).
14. B. Lu, F. Roegiers, L. Y. Jan, Y. N. Jan, *Nature* **409**, 522 (2001).
15. S. C. Schuyler, D. Pellman, *J. Cell Sci.* **114**, 247 (2001).
16. M. Segal, K. Bloom, *Trends Cell Biol.* **11**, 160 (2001).
17. M. Bienz, *Nature Cell Biol.* **3**, E67 (2001).
18. K. Bloom, *Curr. Biol.* **11**, R326 (2001).
19. D. Liakopoulos, J. Kusch, S. Grava, J. Vogel, Y. Barral, *Cell* **112**, 561 (2003).
20. R. K. Miller, M. D. Rose, *J. Cell Biol.* **140**, 377 (1998).
21. L. Lee *et al.*, *Science* **287**, 2260 (2000).
22. K. Akong, B. McCartney, M. Peifer, *Dev. Biol.* **250**, 71 (2002).
23. D. L. Jones *et al.*, in preparation.
24. J. Hulsken, W. Birchmeier, J. Behrens, *J. Cell Biol.* **127**, 2061 (1994).

25. We thank E. Wieschaus, M. Bienz, A. Spradling, T. Uemura, T. Kaufman, H. Oda, the Bloomington Stock Center, and the Developmental Studies Hybridoma Bank for stocks and antibodies. We also thank T. Mahowald, J. Nelson, A. Barth, and Fuller lab members for critical reading of the manuscript and discussions. Y.M.Y. is a Japan Society for the Promotion of Science fellow, and D.L.J. is a Lilly fellow of the Life Sciences Research Foundation. Supported by NIH grant 1P01 DK53074 subproject 4 (M.T.F.).

Supporting Online Material

www.sciencemag.org/cgi/content/full/301/5639/1547/DC1
Materials and Methods
Fig. S1
Table S1
References

9 June 2003; accepted 29 July 2003

Orientation of Asymmetric Stem Cell Division by the APC Tumor Suppressor and Centrosome

Yukiko M. Yamashita, D. Leanne Jones, and Margaret T. Fuller

Science **301** (5639), . DOI: 10.1126/science.1087795